Functional profiling of COVID-19 respiratory tract microbiomes

Niina Haiminen[1], Filippo Utro[1], Ed Seabolt[2], and Laxmi Parida[1,*]

[1]IBM T. J. Watson Research Center, Yorktown Heights, NY, USA

[2]IBM Almaden Research Center, San Jose, CA, USA

[*]parida@us.ibm.com

ABSTRACT

In response to the ongoing global pandemic, progress has been made in understanding the molecular-level host interactions of the new coronavirus SARS-CoV-2 responsible for COVID-19. However, when the virus enters the body it interacts not only with the host but also with the micro-organisms already inhabiting the host. Understanding the virus-host-microbiome interactions can yield additional insights into the biological processes perturbed by the viral invasion. Here we present a framework for comparative functional analysis of microbiomes, the results from which can lead to new hypotheses on the host-microbiome interactions in healthy versus afflicted cohorts. We carry out a functional analysis of previously published RNA sequencing data of bronchoalveolar lavage fluid from eight COVID-19 patients, twenty-five community-acquired pneumonia patients, and twenty healthy controls. The resulting microbial functional profiles and their top differentiating features clearly separate the cohorts. We also detect differentially abundant microbiome pathway signatures in COVID-19 compared to both the community-acquired pneumonia and healthy cohorts. By utilizing randomization to evaluate the significance of the findings, we highlight pathways with altered abundance in COVID-19 respiratory tract microbiomes, including decreased lipid and glycan metabolism.

Background

An impressive number of scientific studies have rapidly been published on the genomics and molecular-level host interactions of the new coronavirus SARS-Cov-2[1] of reported bat origin,[2] responsible for the COVID-19 disease pandemic. Additionally, understanding changes in the microenvironment within the host can yield insights into related biological processes perturbed by the virus. An increase in opportunistic organisms and an enhanced capacity for nucleotide and amino acid biosynthesis and carbohydrate metabolism has been associated with increased SARS-CoV-2 presence in fecal microbiomes.[3] It has been suggested that gut microbiota could contribute to the pathology of the gut-lung axis during COVID-19.[4] The respiratory microbiome members during the respiratory virus SARS-CoV-2 infection have also been examined.[1,5–7] Previous studies on

the respiratory tract microbiome during other pathogen infections have examined its predictivity of clinical outcomes, and associated potential probiotic interventions.[8–12]

To better understand the role of the respiratory microbiome in COVID-19, we introduce a *functional* analysis, as opposed to taxonomic naming, of recently published metatranscriptomes[5] from bronchoalveolar lavage fluid (BALF) of COVID-19 patients, healthy subjects, and community-acquired pneumonia (CAP) cases. While Shen et al.[5] focused on the SARS-Cov-2 genomes and taxonomic profiling of the microbiomes, here we perform global functional profiling to characterize altered biological processes the respiratory tract microbiomes. The robust comparative analysis presented here was designed to highlight consistent differences in COVID-19 patient microbiomes compared to both community-acquired pneumonia and healthy control samples.

Results

Functional profiling framework

The overall analysis workflow is depicted in Fig. 1A. The total RNA sequencing reads were first trimmed and filtered, followed by translation and functional classification with PRROMenade[13] against a vast amino acid sequence collection of 21 million bacterial and viral protein domains from the IBM Functional Genomics Platform,[14] annotated with KEGG enzyme codes (EC) from a corresponding functional hierarchy[15] (see Supplemental Fig. S1 for filtering results). Post-processing and robust rank-based RoDEO[16] projection onto a unified scale was performed to make the resulting functional profiles comparable.

Microbiome functional profiles cluster by cohort

While the individual functional profiles vary, a robust comparative analysis reveals specific functions that are consistently altered between cohorts (Supplemental File S1 shows a Krona[17] visualization of each sample). The read counts assigned at various functional hierarchy levels (Supplemental Fig. S2) were pushed down to the leaf level, and very low abundant features were removed for subsequent analyses (see Methods).

Multi-dimensional scaling of pairwise Spearman distances between the samples separates the COVID-19 cohort, while CAP samples are located between healthy and COVID-19 samples (Fig. 1B). A significant difference between the functional profiles was observed between the COVID-19, CAP, and healthy control cohorts according to the PERMANOVA test ($p \leq 0.0001$). Functional profiling separated the cohorts with a similar score as taxonomic profiling (functional profiling $R^2 = 0.06$ vs. taxonomic profiling by Shen et al[5] $R^2 = 0.07$).

Differentially abundant features distinguish COVID-19 samples

The RNA sequencing data had varying total number of reads and human content per sample (Supplemental Fig. S1). Therefore we used RoDEO[16] to project the functional profiles onto a robust uniform scale. To examine the most differentiating features for COVID-19 versus the other cohorts, we extracted 30 top-ranked features from the COVID vs. CAP comparison and from the COVID vs. healthy controls comparison. We then considered the union of the feature sets, resulting in 44 EC features.

When clustering the samples using the top differentiating features, the COVID-19 samples are grouped together and separate from the other cohorts, except for sample 4 (Fig. 2). While the examined 44 features were selected as those differentiating COVID-19 from CAP and healthy controls, they also separate the healthy control samples from all others; the healthy controls cluster tightly together. The results also demonstrate that the samples do not merely cluster by the total number of input reads or the fraction of functionally annotated microbial reads, since those measures vary within cohorts (Supplemental Fig. S1). The CAP patient samples were collected from different hospital sources, prior to the current pandemic, and represent pneumonia cases with various viruses detected in the sequencing data[5] (e.g. enterovirus, influenza virus, rhinovirus), possibly contributing to the greater variability between their microbiome functional profiles.

The COVID-19 samples have more abundant EC features including (see bottom left feature cluster in Fig. 2) 1.2.4.1 "Pyruvate dehydrogenase", 4.1.1.20 "Diaminopimelate decarboxylase", 1.17.4.1 "Ribonucleoside-diphosphate reductase", 1.8.1.4 "Dihydrolipoyl dehydrogenase", 3.6.3.25 "Sulfate-transporting ATPase", and 4.2.3.5 "Chorismate synthase", mapping to various amino acid, carbohydrate, energy, and nucleotide metabolism pathways. Among those features that are less abundant in COVID-19 (second feature cluster from the bottom in Fig. 2) are 1.2.1.41 "glutamate-5-semialdehyde dehydrogenase", 3.2.1.14 "chitinase", 3.2.1.28 "alpha,alpha-trehalase", 1.4.3.5 "pyridoxal 5'-phosphate synthase", 2.3.1.20 "diacylglycerol O-acyltransferase", 2.6.1.1 "aspartate transaminase", 3.4.11.2 "membrane alanyl aminopeptidase", 3.4.11.5 "prolyl aminopeptidase", 3.6.1.12 "dCTP diphosphatase", mapping to amino acid, carbohydrate, cofactor and vitamin, lipid, and nucleotide metabolism pathways. See also Supplemental Fig. S3 for a scatter plot of the average change per EC in COVID-19 compared to CAP and healthy cohorts.

Altered lung microbiome pathways indicated in COVID-19

In order to systematically examine the detected features against functional pathways, all the EC features were considered against their corresponding pathways from the KEGG metabolic pathway mapping.[15]. Pathway scores (mean abundance change in COVID-19) were computed using all the detected EC features per pathway (see Supplemental Fig. S4 and Methods). To contrast the observed scores against a background distribution, the sample labels were randomly permuted multiple times and the resulting pathway scores computed, see Fig. 3. An empirical p-value per pathway was then computed using the obtained random background distribution. Sixteen pathways were detected as significantly lower ($p < 0.01$) and two pathways as significantly higher in COVID-19.

Among the pathways that were lower in COVID-19, see Fig. 3, several are related to glycan biosynthesis and metabolism (e.g. glycosaminoglycan degradation) and lipid metabolism (e.g. sphingolipid metabolism). A connection between decreased presence of host glycosaminoglycan heparan sulfate modifying bacteria and increased COVID-19 susceptibility has recently been suggested.[18] Sphingolipids are important components of biomembranes, mediating signal transduction and immune activation processes, and they have been shown to decrease in COVID-19 patient sera.[19] The differentially abundant functions and pathways can suggest novel host-microbiome interactions to be examined further.

Discussion

Analyzing COVID-19 respiratory tract metatranscriptomes from a functional perspective offers an additional view into their differences from healthy controls and from subjects with community-acquired pneumonia. The comparative approach taken here aims to mitigate possible experimental variation and resulting biases within individual samples, by focusing on detecting robust and consistent differences in the detected microbial functions. As a result, we identify both enzyme code features and metabolic pathways that differentiate COVID-19 respiratory tract microbiomes from healthy control and community-acquired pneumonia samples. The resulting functional profiles distinguish COVID-19 samples from others, similarly to the original taxonomy-based analysis of the community members.[5]

By employing a randomization approach, we evaluated the significance of the detected differentially abundant pathways. Sixteen pathways showed significantly ($p < 0.01$) lower abundance in COVID-19 compared to the other cohorts, and two pathways higher abundance. Even with a more stringent threshold ($p < 0.0001$) four pathways appear down in COVID-19. Several decreased pathways were related to glycan and lipid metabolism, including sphingolipid metabolism; sphingolipids have been shown to decrease in COVID-19 patient sera.[19] Additionally, related to the decreased glycosaminoglycan degradation pathway, a link between decreased presence of host glycosaminoglycan heparan sulfate modifying bacteria and increased COVID-19 susceptibility has recently been suggested.[18] The differentially abundant functions and pathways can suggest novel host-microbiome interactions to be examined further.

This computational study has limitations including small sample size and overall variation in the sampled microbiomes, possibly due to subject lifestyles, location, and clinical characteristics including different stages and severity of disease. Without related clinical data, connections between administered therapies and detected microbiome differences also remain elusive.

The observations from this functional analysis call for further in-depth research on microbial functions and host-microbiome interactions, by connecting clinical data with microbiome sequencing. This protein domain focused amino acid matching approach supports the profiling of functions performed by known and potentially unknown organisms yet to be characterized.[20] Examining metatranscriptomic sequencing reads with the lens of functional annotation can yield additional insights into disease-related microbiome alterations.

Methods

Sequence data and functional database

The recently published bronchoalveolar lavage fluid (BALF) metatranscriptomic sequencing data[5] of 8 COVID-19 patients, 20 healthy controls (HC), and 25 cases of community-acquired pneumonia (CAP) were obtained from the National Genomics Data Center (accession PRJCA002202).[21] Pre-processing included TrimGalore[22] adapter and quality trimming (–length 50 –trim-n –max_n 10), and poly-A trimming performed with BBduk[23] (trimpolya=10, minlength=50). The reads were filtered against human (GCF_000001405.39), the PhiX sequencing control (GCF_000819615.1), and the SARS-CoV-2 virus (NC_045512.2) with BBsplit[23] (ambiguous=random, ambiguous2=split). The paired reads were processed separately, individual reads that

did not match the human, PhiX, or SARS-CoV-2 genomes (278k to 50.7M reads per sample) were retained for the microbial community functional annotation (see Supplemental Fig. S1 for the filtering results).

The KEGG Enzyme Nomenclature (EC) reference hierarchy[15] was used as the functional annotation tree. The EC numbers define a four-level hierarchy. For example, 1.5.1.3. = "Dihydrofolate reductase" is a fourth (leaf) level code linked to top level code 1 = “Oxidoreductases”, via 1.5. = “Acting on the CH-NH group of donors" and 1.5.1 = “With NAD+ or NADP+ as acceptor”. A PRROMenade[13] database search index was constructed using the KEGG hierarchy and a total of 21.2M bacterial and 53k viral annotated protein domain sequences (of minimum length 5 AA), obtained on June 6, 2020 from the IBM Functional Genomics Platform[14] (previously known as OMXWare). An earlier release of the bacterial domain data has been discussed previously in conjunction with PRROMenade indexing.[13]

Functional annotation and analysis

Metatranscriptomic sequencing reads were annotated with PRROMenade by locating the maximal length exact match for each read, and processed as described previously.[13] Minimum match length cutoff of 11 AA (corresponding to 33 nt) was employed. Classified (non-root) read counts (6.8k to 11.5M per sample, see Supplemental Fig. S1–S2) were post-processed to summarize the counts at the leaf level of the functional hierarchy. Leaf nodes contributing $\geq 0.05\%$ of total annotated reads in at least one sample were retained, resulting in 633 leaf nodes to include as the features of the functional profiles. Multidimensional scaling (Matlab function cmdscale, $p = 2$) and permutational multivariate analysis of variance (f_permanova, $iter = 100,000$, from the Fathom toolbox[24] for Matlab) were applied on pairwise Spearman’s distances (Fig. 1B).

Subsequently, the profiles were processed with RoDEO[16] ($P = 10$, $I = 100$, $R = 10^7$) for robust comparability. The per-sample parameter P' was determined according to the number of annotated reads as previously described (in Supplementary File 2 by Klaas et al.[25]). A two-sample Kolmogorov-Smirnov test (kstest2 in Matlab) was applied to identify differentially abundant features between COVID-19 samples and CAP, healthy control samples. Features were ordered by p-value and top features selected for average linkage hierarchical clustering using the Euclidean distance (Fig. 2).

Pathway analysis

The KEGG[15] metabolic pathway maps were utilized to link functions with pathways, and the pathways were analyzed for changes between COVID-19 and CAP, HC. The pathways were evaluated for average abundance change as follows. Let a_i be the mean RoDEO abundance of EC feature i for COVID-19 samples, b_i for CAP samples, and c_i for HC samples. The feature score is defined as $fs_i = ((a_i - b_i) + (a_i - c_i))/2$, positive values indicating higher abundance in COVID-19. Pathway score $ps_j = mean\{fs_{EC_j(1)}, fs_{EC_j(2)}, ..., fs_{EC_j(k)}\}$ was computed using the set of features, EC_j, that map to the pathway j (considering only pathways with $k \geq 2$).

To evaluate significance of the results, the sample labels were randomly permuted 10,000 times and ps_j of each pathway computed. The pathway scores across permutations were combined as the background distribution (Supplemental Fig. S4). An empirical p-value for pathway score $ps_j = x$ was computed as $p(x) = (r+1)/(n+1)$, where n is the total number of pathway

scores across all the randomizations, and r is the number of pathway scores with values $< x$ (for low pathway scores) or $> x$ (for high pathway scores).

Author contributions

N.H. and F.U. conducted the experiments, analyzed the results and wrote the manuscript. E.S. provided reference data from the IBM Functional Genomics Platform. N. H. and L.P. conceived the study and analyzed the results. All authors reviewed the manuscript.

Competing interests

The PRROMenade methodology is associated with patent applications currently pending review at the USPTO.

References

1. Zhou, P. *et al.* A pneumonia outbreak associated with a new coronavirus of probable bat origin. *Nature* **579**, 270–273 (2020).
2. Andersen, K. G., Rambaut, A., Lipkin, W. I., Holmes, E. C. & Garry, R. F. The proximal origin of SARS-CoV-2. *Nat Medicine* **26**, 450–452 (2020).
3. Zuo, T. *et al.* Depicting SARS-CoV-2 faecal viral activity in association with gut microbiota composition in patients with COVID-19. *Gut* (2020).
4. Yang, T. *et al.* Gnotobiotic Rats Reveal That Gut Microbiota Regulates Colonic mRNA of Ace2, the Receptor for SARS-CoV-2 Infectivity. *Hypertension* **76** (2020).
5. Shen, Z. *et al.* Genomic Diversity of Severe Acute Respiratory Syndrome–Coronavirus 2 in Patients With Coronavirus Disease 2019. *Clin. Infect. Dis.* (2020).
6. Chen, L. L. *et al.* RNA based mNGS approach identifies a novel human coronavirus from two individual pneumonia cases in 2019 Wuhan outbreak. *Emerg. Microbes & Infect.* **9**, 313–319 (2020).
7. Wu, F. *et al.* A new coronavirus associated with human respiratory disease in China. *Nature* **579**, 265–269 (2020).
8. Hanada, S., Pirzadeh, M., Carver, K. Y. & Deng, J. C. Respiratory viral infection-induced microbiome alterations and secondary bacterial pneumonia. *Front. Immunol.* **9**, 2640 (2018).
9. Mendez, R., Banerjee, S., Bhattacharya, S. K. & Banerjee, S. Lung inflammation and disease: A perspective on microbial homeostasis and metabolism. *IUBMB Life* **71**, 152–165 (2019).
10. Dickson, R. P. *et al.* Lung microbiota predict clinical outcomes in critically ill patients. *Am. J. Respir. Critical Care Medicine* **201**, 555–563 (2020).
11. Zolnikova, O., Komkova, I., Potskherashvili, N., Trukhmanov, A. & Ivashkin, V. Application of probiotics for acute respiratory tract infections. *Italian J. Medicine* **12**, 32–38 (2018).

12. Fanos, V., Pintus, M. C., Pintus, R. & Marcialis, M. A. Lung microbiota in the acute respiratory disease: from coronavirus to metabolomics. *J Pediatr Neonat Individ. Med* **9**, e090139 (2020).

13. Utro, F. *et al.* Hierarchically labeled database indexing allows scalable characterization of microbiomes. *iScience* **23** (2020).

14. Seabolt, E. *et al.* IBM Functional Genomics Platform, A Cloud-Based Platform for Studying Microbial Life at Scale. *IEEE/ACM Transactions on Comput. Biol. Bioinforma.* (2020).

15. Kanehisa, M., Furumichi, M., Tanabe, M., Sato, Y. & Morishima, K. KEGG: new perspectives on genomes, pathways, diseases and drugs. *Nucleic Acids Res* **45**, D353–D361 (2017).

16. Haiminen, N. *et al.* Comparative exomics of Phalaris cultivars under salt stress. *BMC Genomics* **15 Suppl 6**, S18 (2014).

17. Ondov, B., Bergman, N. & Phillippy, A. Interactive metagenomic visualization in a web browser. *BMC Bioinformatics* **12** (2011).

18. Martino, C. *et al.* Bacterial modification of the host glycosaminoglycan heparan sulfate modulates SARS-CoV-2 infectivity. *bioRxiv* DOI: 10.1101/2020.08.17.238444 (2020).

19. Shen, B. *et al.* Proteomic and Metabolomic Characterization of COVID-19 Patient Sera. *Cell* **182**, 59–72.e15 (2020).

20. Kaufman, J. H. *et al.* Insular microbiogeography: Three pathogens as exemplars. *Curr Issues Mol Biol* **36**, 89–108 (2020).

21. National Genomics Data Center Members and Partners. Database Resources of the National Genomics Data Center in 2020. *Nucleic Acids Res.* **48**, D24–D33 (2020).

22. Krueger, F. TrimGalore. https://github.com/FelixKrueger/TrimGalore.

23. Bushnell, B. BBtools. https://sourceforge.net/projects/bbmap/.

24. Jones, D. L. Fathom Toolbox for MATLAB: software for multivariate ecological and oceanographic data analysis. https://www.usf.edu/marine-science/research/matlab-resources/index.aspx/ (2017).

25. Klaas, M. *et al.* Transcriptome characterization and differentially expressed genes under flooding and drought stress in the biomass grasses Phalaris arundinacea and Dactylis glomerata. *Annals Bot.* **124**, 717–730 (2019).

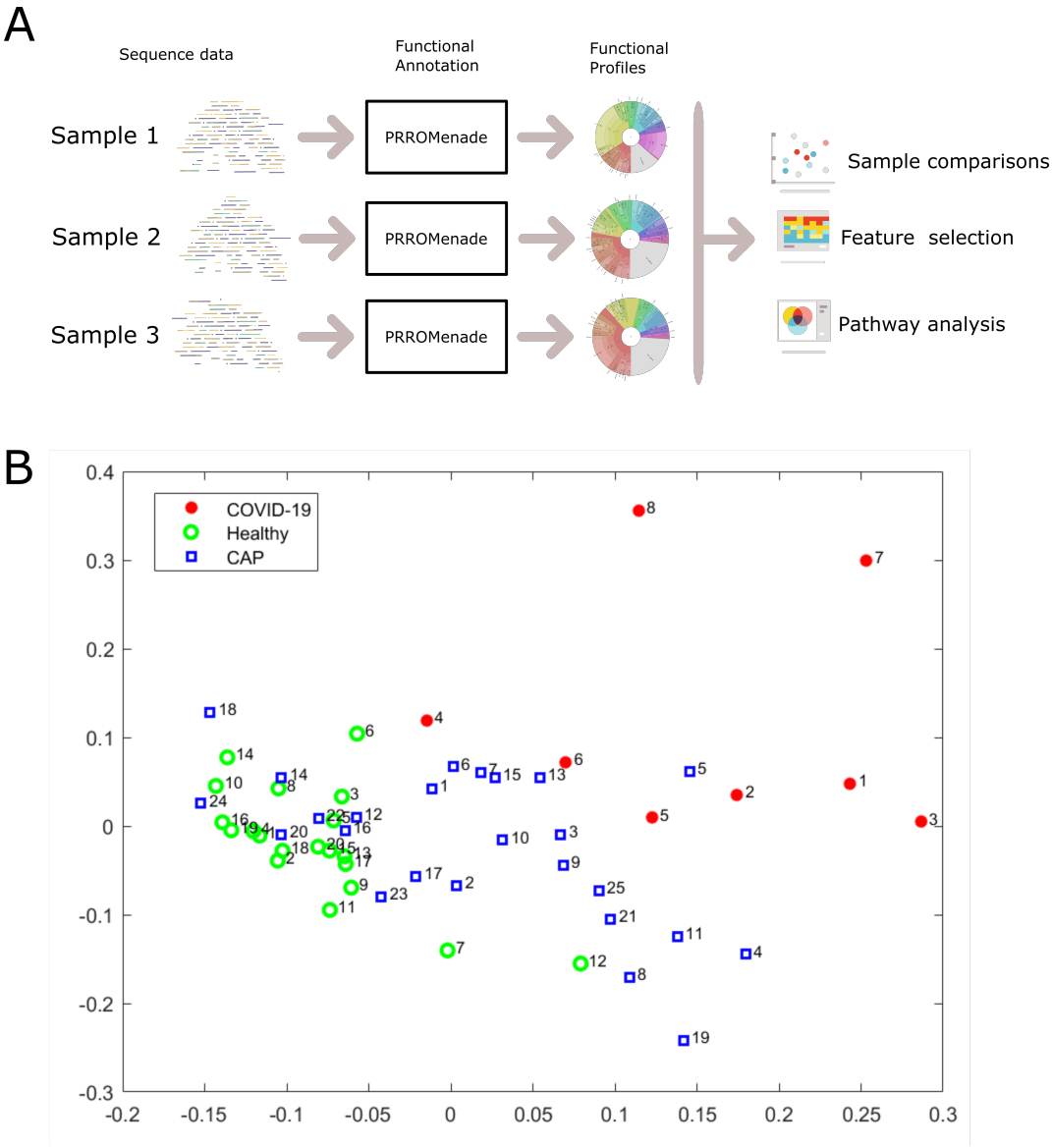

Figure 1. **A**. Overall analysis workflow. Each microbiome sequencing sample is annotated with PRROMenade, utilizing labeled reference data from the IBM Functional Genomic Platform. The resulting functional profiles are visualized and compared in downstream analyses. **B**. Multidimensional scaling of the functional profiles using the Spearman distance. Each sample is represented by a marker colored by cohort and labeled by the sample number within that cohort.

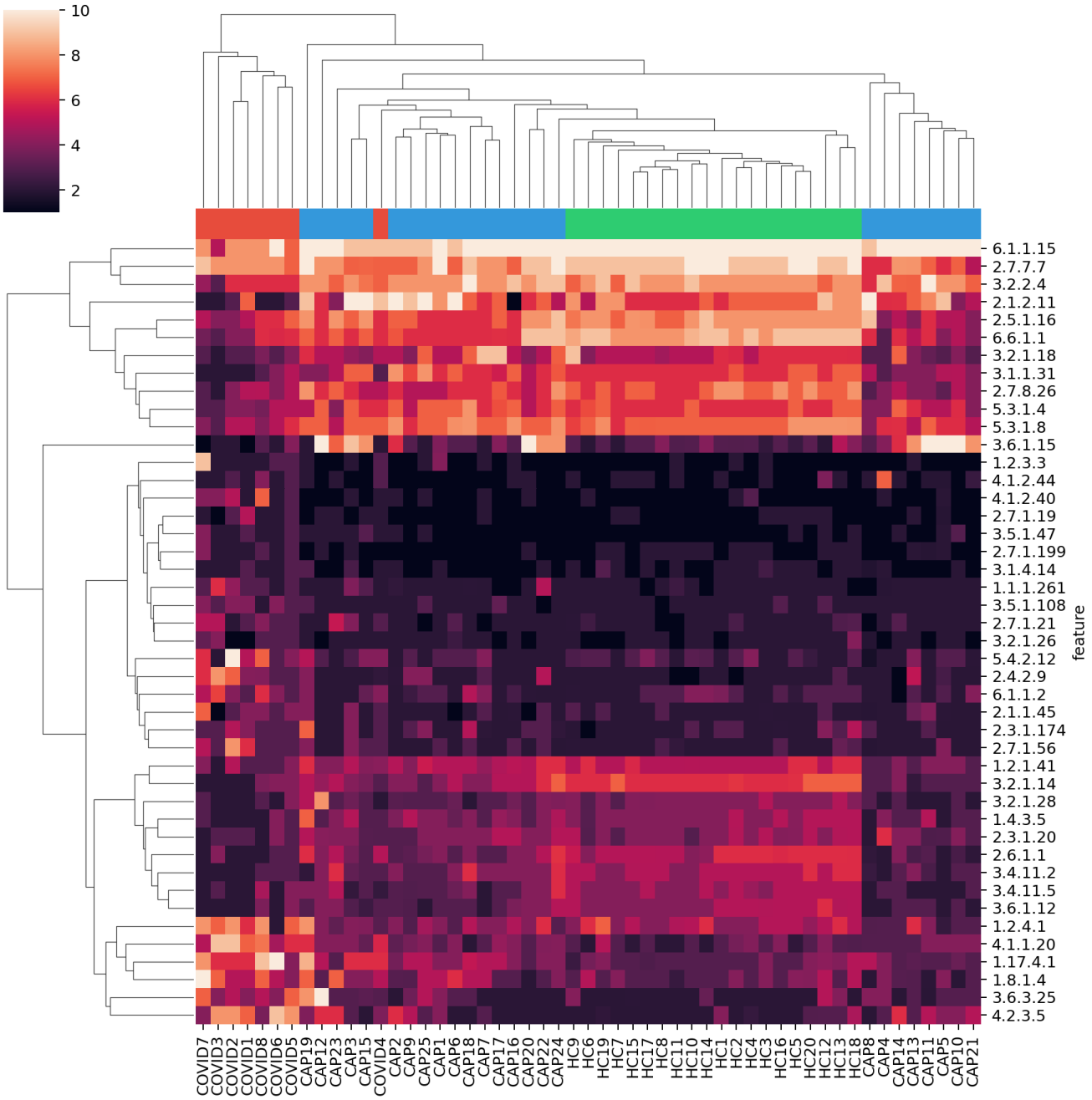

Figure 2. RoDEO processed EC abundance values (10 denotes highest possible value), for 44 features differentiating COVID-19 from community-acquired pneumonia and healthy controls. Columns and rows are ordered independently by hierarchical clustering of features and samples. The colors attached to the dendrogram on top reflect the cohort labels: red = COVID-19, blue = CAP, green = healthy control.

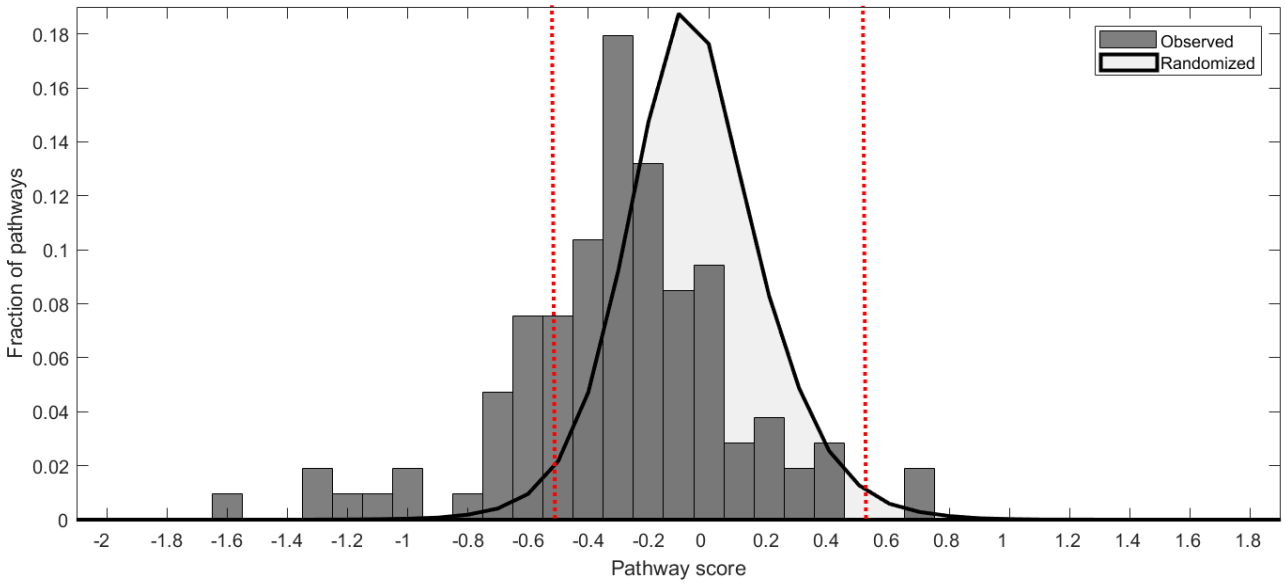

Pathway name	p-value	+/-	#EC	Type
Tropane, piperidine and pyridine alkaloid biosynthesis	9.4e-07	-	2	Biosynthesis of other secondary metabol.
Carbapenem biosynthesis	1.0e-05	-	2	Biosynthesis of other secondary metabol.
Glycosphingolipid biosynth. - globo and isoglobo series	1.7e-05	-	2	Glycan biosynthesis and metabolism
Novobiocin biosynthesis	8.6e-05	-	3	Biosynthesis of other secondary metabol.
Sphingolipid metabolism	0.0002	-	5	Lipid metabolism
Ether lipid metabolism	0.0003	-	3	Lipid metabolism
Other glycan degradation	0.0004	-	4	Glycan biosynthesis and metabolism
Glycerolipid metabolism	0.0015	-	5	Lipid metabolism
Other types of O-glycan biosynthesis	0.0053	-	2	Glycan biosynthesis and metabolism
Fluorobenzoate degradation	0.0055	-	2	Xenobiotics biodegradation and metab.
Glycosaminoglycan degradation	0.0058	-	3	Glycan biosynthesis & metabolism
Caffeine metabolism	0.0059	-	3	Biosynth. other secondary metabolites
One carbon pool by folate	0.0067	-	11	Metabolism of cofactors and vitamins
Arachidonic acid metabolism	0.0086	-	3	Lipid metabolism
beta-Alanine metabolism	0.0094	-	4	Metabolism of other amino acids
Atrazine degradation	0.0099	-	2	Xenobiotics biodegradation and metab.
Acarbose and validamycin biosynthesis	0.0040	+	2	Biosynthesis of other secondary metabol.
Polyketide sugar unit biosynthesis	0.0040	+	2	Metabolism of terpenoids and polyketides

Figure 3. The randomized background distribution (shaded area under the black curve) of pathway scores across permutations of sample labels, and the observed pathway scores (bars) are shown. The empirical p-value threshold < 0.01 is also marked (red dashed lines). Eighteen differential pathways in COVID-19 samples are highlighted in the table. The direction of the change in COVID-19 (+/-), the number of associated EC features per pathway detected from functional profiling (#EC), and the pathway type are also shown.